Defence Science Journal, Vol. 74, No. 4, July 2024, pp. 460-468, DOI : 10.14429/dsj.74.19198

Experimental and Numerical Investigation of Bodywork Effect on High-Hardness Armour Steel Against a 7.62 x 51 mm NATO Ball M80 Projectile

Gavhane Viraj Vijaykumar[#,*], Anshul Sharma[#] and Srinivasa Rao Gorrepati[$]

[#]*Mahindra Defence Systems Limited–Land Systems, Palwal – 121 102, India*
[$]*Amity Institute of Defence Technology, Amity University, Noida – 201 303, India*
[*]*E-mail: viraj.gavhane01@gmail.com*

ABSTRACT

Small arms ammunition like the 5.56×45 mm NATO Ball and 7.62×51 mm NATO Ball projectiles constitute a significant threat to light armoured vehicles. These vehicles are mostly comprised of single-layered metallic high-hardness steel armour, but as an essential vehicle design feature, mild steel bodywork is externally mounted in certain areas for fenders, toolkit boxes, storage boxes, etc. over the main armour, i.e., high-hardness steel armour. These are necessary design features of vehicles, so they can't be neglected regarding ballistic protection against threats. Also, to provide better ballistic protection in up-armoured vehicles, armour consisting of high-hardness steel armour is integrated or mounted just behind the existing bodywork of the car. Thus, this paper experimentally and numerically investigated the "bodywork effect," which is also called the "K-effect," and found that the configuration where the bodywork of mild steel is placed in front of high-hardness steel armour plate failed to provide better ballistic protection against the 7.62×51 NATO Ball M80 projectile fired at 0° angle of impact with a velocity of 833±20m/s from 10 m distance. However, the single high-hardness armour steel plate provided better ballistic protection than the configuration consisting of bodywork. For the validation of the experimental investigations, the arrangements were numerically simulated. The main aim of this work was to check the bodywork effect against this particular projectile and investigate factors contributing to the phenomenon.

Keywords: Projectile; Mild steel plate; High-hardness steel; Armox 500T; Perforation; Body effect

1. INTRODUCTION

The primary threats against the Light Armoured Vehicles are 5.56×45 mm and 7.62×51 mm NATO Ball cartridges, classified as small arms ammunition, precisely, as a Level 1 threat according to STANAG 4569[1]. Most of the light armoured vehicles are made up of main armour, i.e., single metallic high-hardness steel plate, but as part of important vehicle design, extra bodywork of mild steel is added over in some regions of the vehicle, e.g., fenders, toolkit boxes, storage boxes, etc. When improving the ballistic protection of the up-armoured vehicles against small arms ammunition, an armour kit is integrated into the existing vehicle's bodywork. The integration of the armour kit is such that it is not visible from the outside. The armour kit comprises high-hardness steel plates because of their low cost, reliability, ease of production, and, most importantly, their good ballistic performance. Steel armour is consistently used in the tempered martensitic microstructure form after heat treatment. It involves hardening the steel to increase its resistance to projectile penetration and then tempering it to make it tougher and increase its ability to absorb energy from impacting projectiles.

Numerous investigations on the penetration and perforation of metallic plates by various projectiles have been done during the last few decades. Numerous articles have been published that provide thorough assessments of this topic[2-9]

This issue is challenging because it considers various variables, including projectile impact velocities and nose shapes, nonlinearities in target materials and geometries, and strain rate sensitivity after impact. However, Numerous research investigations indicate that various variables, including impact velocity, projectile nose shape, projectile diameter to plate thickness ratio and other factors, affect the deformation and failure modes of metallic plates.

Metallic plates that are subjected to projectile contact can break down in a variety of ways, such as Petalling [10], plugging[10], bulging[11], ductile holes[12], radial cracking[12], and spalling[12]. The fracture mechanisms observed in a 6 mm thick monolithic Armox 500T target fired with 7.62×51 mm NATO FMJ M80 projectiles having a brass jacket and lead core revealed that the target failed to owe ductile hole formation and petalling for impact velocities greater than the target's Ballistic Limit Velocity and that a bulge was seen at the target's back face for impacts with rates lower than the target's Ballistic Limit Velocity[13]. Conical projectile tends to fail the target in the form of petalling[8-14], and blunt Projectile tends to fail the target in the form of plugging[8,15].

Ideally, the addition of the thin mild steel, i.e., bodywork, in front of the high-hardness steel armour plate with separation

Received : 27 June 2023, Revised : 18 October 2023
Accepted : 14 November 2023, Online published : 24 July 2024

Table 1. Chemical composition of ARMO×500T

Material	C (max %)	Si (max %)	Mn (max %)	P (max %)	S (max %)	Cr (max %)	Ni (max %)	Mo (max %)	B (max %)
Armox 500T	0.32	0.40	1.20	0.010	0.003	1.0	1.80	0.70	0.005

Table 2. Mechanical properties of ARMOX 500T

Hardness (BHN)	Impact toughness (J)	Yield strength (N/mm^2)	Tensile strength (N/mm^2)	Elongation A_5 (%)	Elongation A_{50} (%)
480 - 540	32J/-40°C	1250	1450 - 1750	8	10

Table 3. 7.62 x 51 mm M80 projectile properties

Ammunition	Core and jacket	Cartridge length (mm)	Core weight (g)	Velocity (m/s)
7.62 X 51 mm M80	Lead Core, Copper Jacket	71.12	9.65	833 ± 20 m/s

in between should provide better ballistic performance, but this is leading to the "bodywork effect," where this configuration, i.e., bodywork plus armour plate, is providing less ballistic protection as compared to a single high-hardness steel armour plate.

This so-called "bodywork effect" has previously been observed in the following investigations: Coghe F*., et al.*, experimentally investigated the bodywork effect because the projectile tends to flatten after perforating the bodywork, which causes a plugging failure mechanism in the armour plate. The reason behind the plug failure was the erosion of the projectile's brass jacket at the nose, which led to the formation of a blunt steel core at the tip of the projectile[16].

N. Nsiampa*, et al.* investigated the bodywork effect through numerical results. The numerical simulation for the configuration, i.e., bodywork plus 10 mm separation, i.e., air gap plus the armour plate against a full metal jacket FMJ having a steel and lead core with a brass jacket, failed to perforate the armour plate, and no strain localization was observed. Because the brass jacket material at the nose was not wholly eroded as observed in the previous experimental study. In this Numerical simulation, The dynamic behaviour of Armour Steel was characterized with the help of Split Hopkinson Pressure Bar Tests[17].

F. Coghe*, et al.* investigated the bodywork effect through numerical and experimental results, examining the change in geometry of the 5.56×45 mm NATO Ball Bullet (SS109, M855) and 5.56×45 mm M193 Ball Bullet projectile (i.e., the flattening of the projectile's nose as soon as it perforated the thin mild steel bodywork, which led to a change in the stress triaxiality in high-hardness steel armour plate and then resulted in a plugging shear failure mechanism. This was clarified with the help of finite element simulation. The Johnson-Cook Strength and Failure model, along with the Split Hopkinson Pressure Bar (SHPB) test, were used in numerical simulations to understand the behaviour of armour material[18].

It is worth noting that Adiabatic Shear has significant effects on some armour materials, especially high-strength steels, where gains in static material strength qualities are occasionally followed by a decrease in penetrating resistance over specific hardness ranges[19]

Previous research studies did not use of the 7.62×51 mm NATO Ball M80 projectile. Therefore, to check whether this projectile shows the bodywork effect or not, We decided to go further and deeper into the discussion of the bodywork effect with a 7.62×51 mm NATO Ball M80 projectile against the configuration, i.e., thin mild steel bodywork plus Armox 500T armour steel plate with air gap in between.

For the validation of the experimental investigation of the "Bodywork Effect." A numerical simulation using the Johnson-Cook model was carried out to understand the bodywork phenomenon thoroughly.

2. METHODOLOGY

2.1 Material

Armour steel is the preferred material for vehicles' ballistic and blast protection. SSAB, a company based in Sweden, is one of the leading manufacturers of high-strength armour steel. Armox armour steels are extensively used in both the military and civil sectors. Armox Steel is a type of add-on armour used in manufacturing light armoured vehicles, infantry fighting vehicles, and tanks in the defence industry. Armox armour steels are also used in civil applications such as cash-in-transit vehicles, security doors, and protected buildings. Armox 500T steel, out of all the Armox steels, is particularly important to industry because of its excellent ballistic properties. The high hardness of this martensitic steel, which is paired with exceptional toughness and tensile strength, is well recognized. Additionally, the machining of Armox 500T is simple. Armox 500T is appropriate for ballistic and blast protection due to the perfect balance between toughness and hardness[20-22].

The nominal chemical composition of the steel used in this study is listed in Table 1[22]. The mechanical properties of armour steel are presented in Table 2[22].

2.2 Projectile

Ballistic tests were performed with the 7.62 mm × 51 NATO ball M80 (Lead Core, Copper jacket) projectiles. The properties of this projectile are given Table 3[1].

2.3 Numerical Modelling

The numerical simulations used Altair Hypermesh as the

pre-processor and Ansys LS-DYNA as the post-processor. The geometric and material modelling of the target and the projectile were done in the Hypermesh and post-processing was done in LS-DYNA. A 500x500x6.5 mm plate has been modelled as the main high-hardness steel armour. It was meshed with 12960 nos. 8-node hexagonal brick elements and 10 elements across the thickness with a mesh size of 0.65 mm.

According to the Johnson-Cook constitutive relation, the target was simulated as a viscoplastic material. A fully clamped condition was represented by degrees of freedom on the plate edges being arrested. As a load condition, the projectile was given different initial velocities.

Characterizing the behaviour of materials under high strain rate loading conditions is necessary to explain the various physical events that occur during high-velocity impact and penetration. The stress-strain relationship at high strains or various strain rates, as well as the damage and mechanism of failure, are all included in the material behaviour model. It isn't easy to characterize such complex material behaviour in an analytical model. Therefore, complex constitutive materials can be implemented in numerical simulations. Johnson-Cook is a commonly used material model in ballistic penetration research. A visco-plastic model for ductile metals called the Johnson-Cook model considers the effects of strain rate, strain hardening, and heat softening on material behaviour and fracture.

With an empirical relationship for the flow stress, Johnson-Cook expresses the equivalent stress as a function of plastic strain, strain rate, and temperature, denoted by[23].

$$\sigma = \left(A + B{\varepsilon_p}^n\right)\left(1 + C ln{\varepsilon_p}^*\right)\left(1 - {T_H}^m\right) \quad (1)$$

where,

A = yield stress of the material under reference condition
B = Strain hardening constant
n = Strain hardening coefficient
ε_p = Plastic strain
C = Strengthening coefficient of strain rate
$\varepsilon_P^* = \frac{\dot{\varepsilon}}{\dot{\varepsilon}_0}$ = *where,* $\dot{\varepsilon}$ *is plastic strain rate* $\wedge$ $\dot{\varepsilon}_0$ *is reference strain rate*
T_H = homologous temperature = $\{T_H = (T\text{-}T_{room})/(T_{melting} - T_{room})\}$
m = thermal softening constant

A, B, C, n & m are the five material constants. The stress is expressed as a function of ${\varepsilon_p}^*$=1 and T_H =0 in the first pair of brackets. The effects of strain rate and thermal softening are denoted by the formulae in the second and third brackets, respectively.

Johnson and Cook have also given a model that takes failure strain, temperature, and the effects of stress triaxiality to characterize ductile fracture. It is a cumulative damage-fracture model. This model states that damage builds up in the material during plastic straining and that when the damage reaches a critical value, the material immediately breaks. This indicates that until the fracture occurs, the damage has no impact on the stress field. The strain to fracture is expressed as a function of strain rate, temperature, and pressure. Compared to strain rate hardening and thermal softening, the strain hardening parameters D_1, D_2, and D_3 are more critical and should be thoroughly investigated. Since the J-C model predicts instantaneous failure, no strength is left after an element has eroded. Local material damage is determined using the following damage parameter formula:

$$D = \frac{\Delta\varepsilon}{\varepsilon^f} \quad (2)$$

where,

$\Delta\varepsilon$ = Incremental strain
ε^f = Failure strain

$$\varepsilon_f = \left[D_1 - D_2 exp\left(D_3\sigma^*\right)\right]\left[1 + D_4 ln{\varepsilon_P}^*\right]\left[1 + D_5 T_H\right] \quad (3)$$

The dimensionless pressure/stress ratio (σ_* is the ratio of Hydrostatic stress per effective stress) is a measure of triaxiality of the stress state and is defined as

$$\sigma^* = \frac{\sigma_H}{\sigma_{eq}} \quad (4)$$

The damage variable D can have values between 0 and 1, where D = 0 indicates that the material is undamaged and D = 1 suggests that the elements have failed. Mean stress, strain rate, and temperature are functions of the failure strain and damage accumulation.

2.4 Test Setup

In the experimental test setup, as shown in Fig. 1, a projectile is fired from 10 meters towards a target. To measure the velocity of the projectile during its flight, a velocity-measuring device is strategically positioned between the firing point and the target. Finally, to ensure the safe capture of the projectile and prevent any potential hazards, a specialized projectile-catching system is positioned behind the target. This setup enables comprehensive analysis of the projectile's velocity from launch to impact, providing valuable data.

Table 4. Johnson-cook strength parameters

Parameters	Armox 500T armour plate	Mild steel	Lead core	Copper jacket
A(*MPa*)	1372	350	1.00	89.63
B(*MPa*)	835	275	55.55	291.64
n	0.247	0.36	0.098	0.31
C	0.062	0.022	0.230	0.025
m	0.84	1.00	1.00	1.09
Reference	24	25	-	26

Table 5. Johnson cook damage parameters

Parameters	Armox 500 T armour plate	Mild steel	Lead core	Copper jacket
D1	0.0428	0.8	0.002	0.54
D2	2.1521	2.1	0.010	4.88
D3	-2.7575	-0.5	0.006	-3.03
D4	-0.0066	0.0002	0.003	0.014
D5	0.86	0.61	0.00	1.12
Reference	24	25	-	-

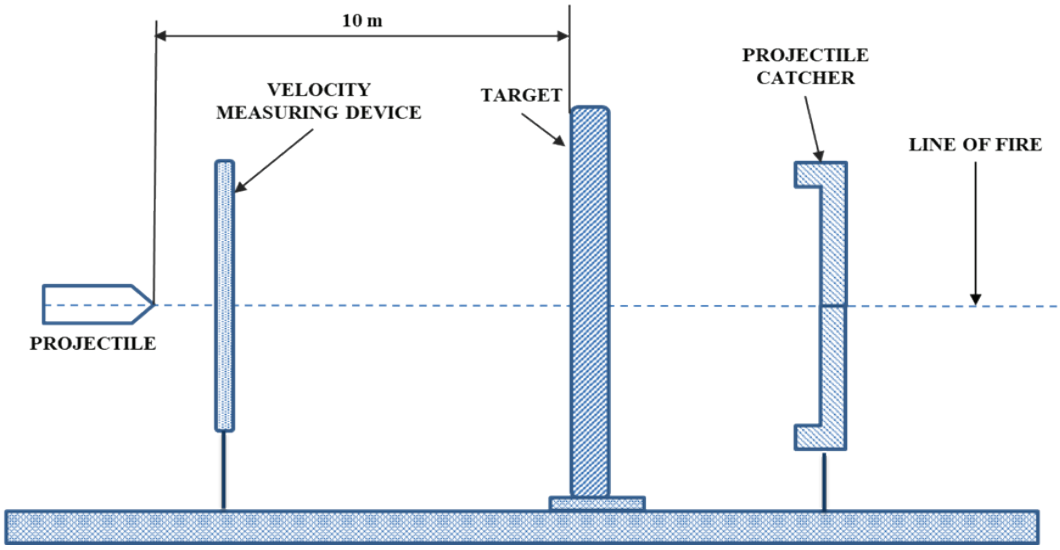

Figure 1. Schematic diagram of test setup.

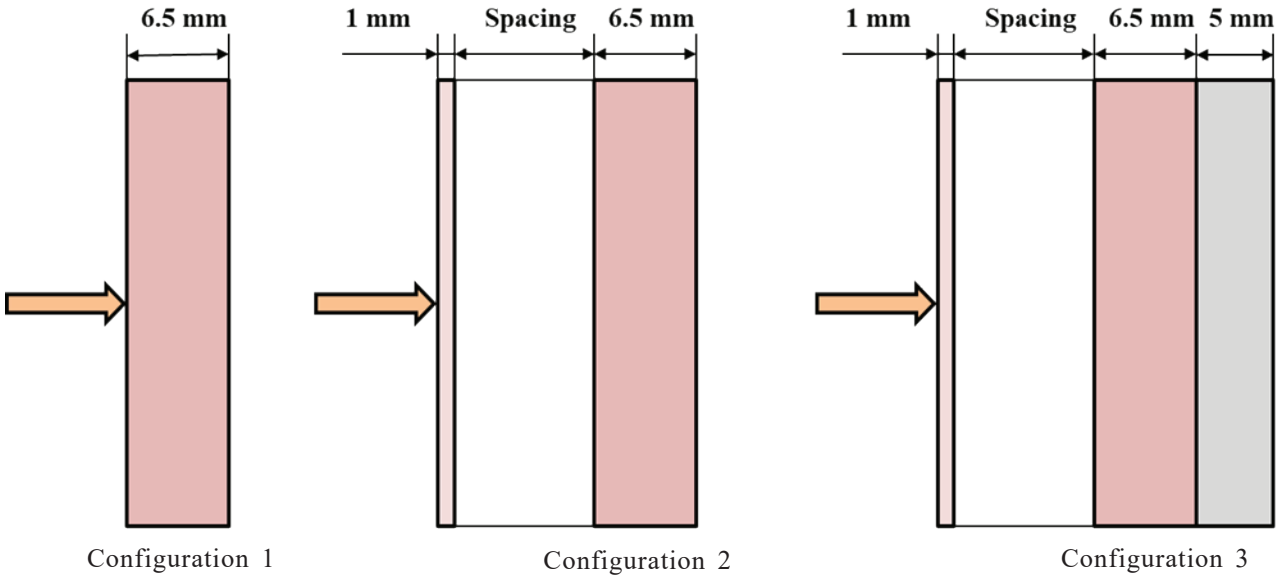

Figure 2. Schematic diagram of three configurations.

Table 6. Experimental results of three configurations

Configuration	Thickness(mm)	Shot number	Impact Angle	Impact velocity (m/s)	Result	Remarks
Configuration 1 (Figure 3 a & b)	6.5 mm	S-1	0°	851.8	No Perforation	Single armour plate did not perforate
		S-2	0°	852.9	No Perforation	Single armour plate did not perforate.
Configuration 2 (Figure 3 c & d)	1mm + 80 mm Spacing + 6.5 mm	S-3	0°	849.5	Perforation	Complete penetration was observed in the Armour Plate.
		S-4	0°	845.1	Perforation	Complete penetration was observed in the Armour Plate.
Configuration 3 (Figure 3 e & f)	1mm + 80 mm Spacing + 6.5 mm + Spall Liner	S-5	0°	848.6	Perforation	The armour plate penetrated, but the shot was blocked by the spall liner.
		S-6	0°	850.3	Perforation	The armour plate penetrated, but the shot was blocked by the spall liner.

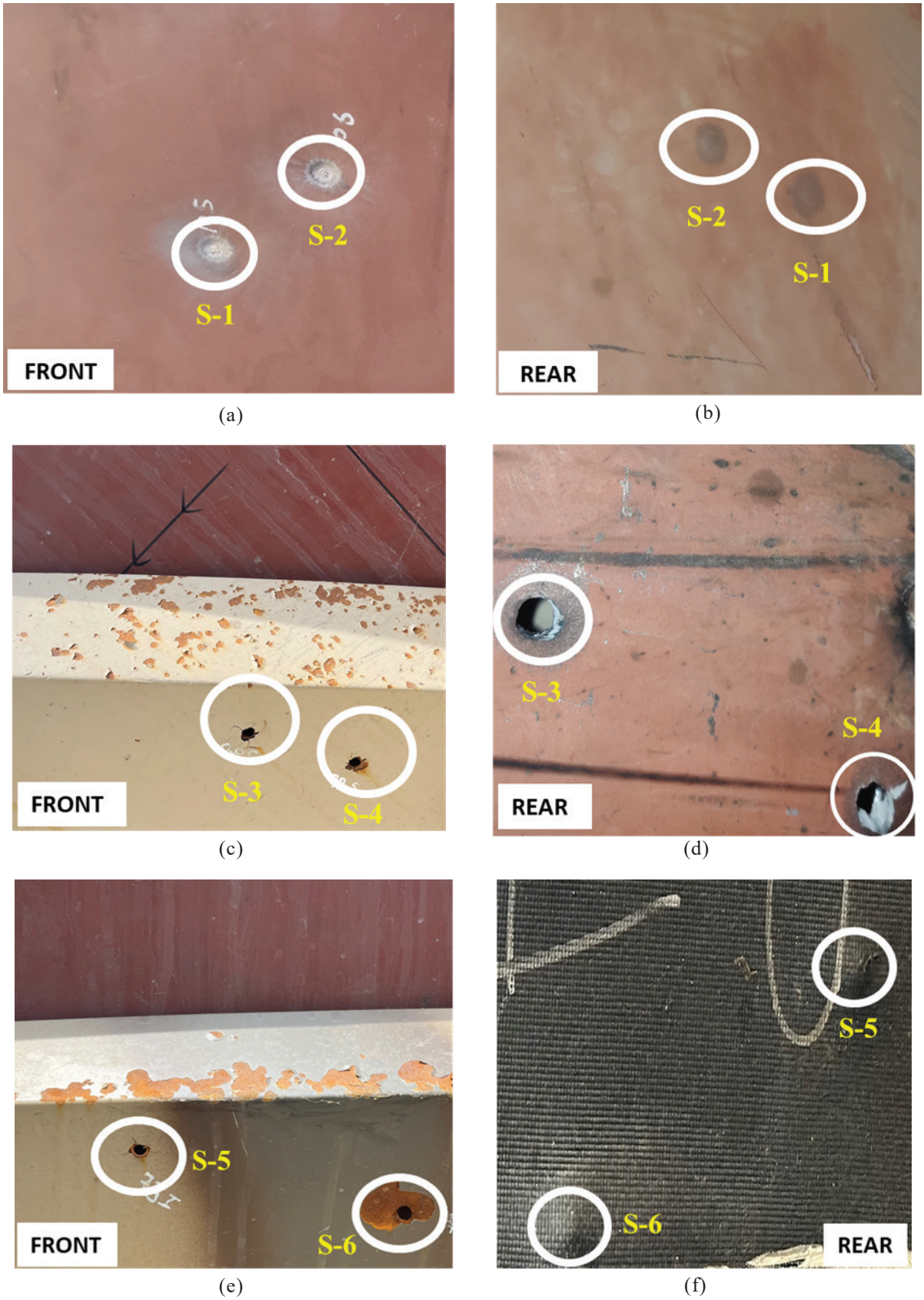

Figure 3. (a) Front view showing two shots fired on Configuration 1; (b) Rear view showing bulge caused by the fired two shots on Configuration 1; (c) Front view showing two shots fired on Configuration 2 caused perforation in the thin mild steel bodywork; (d) Rear view showing perforation caused by the two shots in the high-hardness main armour steel plate; (e) Front view showing perforation in the thin mild steel bodywork caused by the two shots fired on the Configuration 3; and (f) Rear view showing bulge caused by the two shots hit on the spall liner after the perforation of high-hardness main steel armour plate.

3. RESULTS

3.1 Experimental Results

Ballistic tests were conducted for three sample configurations shown in Fig. 2 against the 7.62 x 51 mm NATO Ball M 80 projectile. The findings of the ballistic test procedure are displayed in Table 6.

Three configurations were tested are as follows,

Configuration 1: 6.5 mm High Hardness ARMOX 500T armour steel.

Configuration 2: 1 mm Mild Steel Bodywork + 80 mm Spacing (Air gap) + 6.5 mm High-Hardness Armox 500T armour Steel.

This configuration shows the case for some regions of a vehicle where bodywork is necessarily added or mounted over the main armour as a critical design feature like fenders, toolkit boxes, storage boxes etc. Also for up-armoured vehicles where high-hardness armour steel is integrated into the existing bodywork.

Configuration 3: 1 mm Mild Steel Bodywork + 80 mm Spacing (Air gap) + 6.5 mm High-Hardness Armox 500T armour Steel + 5 mm Spall liner.

A Spall liner was added to check whether it further stops the penetration.

As mentioned in Table 6, Configuration 1 was able to block the shots, and a slight bulge was observed, as seen in Fig. 3(a) and 3(b), respectively. Thus, No perforation was observed in Configuration 1. Complete penetration of configuration 2 was observed where the main armour plate perforated to plugging failure, as seen in Figures 3(c) and 3(d). In Configuration 3, the main armour plate completely penetrated against shots, but the spall liner averted the complete perforation of Configuration 3, as seen in Fig. 3(e) and 3(f).

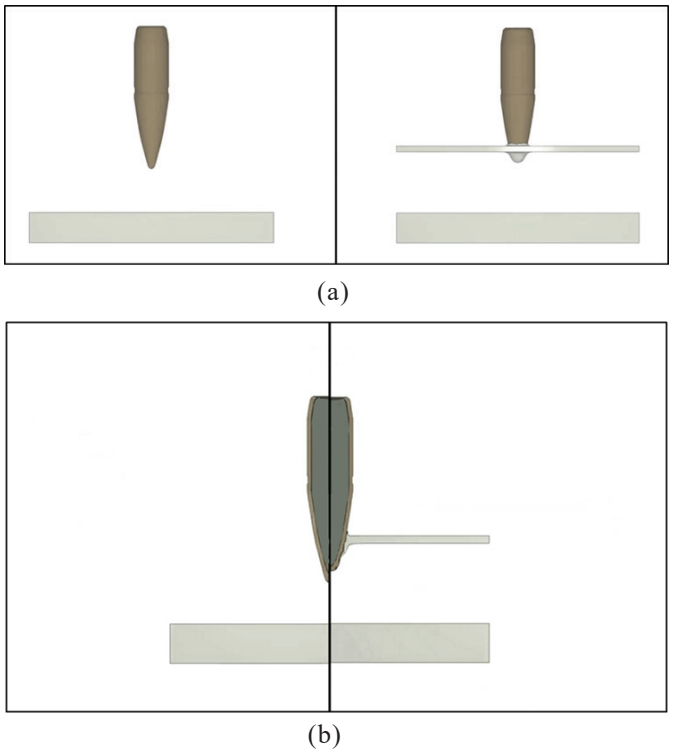

(a)

(b)

Figure 4. (a) Shot fired on Configuration 1 and Configuration 2; and (b): Change in the nose shape of the projectile after perforating the thin mild steel bodywork.

3.2 Numerical Simulation Results

The main of the numerical simulation was to check and validate the bodywork effect and the reasons contributing to it. For the numerical simulation, the materials' Johnson-Cook Strength and Damage/failure parameters were taken from open literature and mentioned in Tables 4 and 5 respectively [24-26].

We have only considered Configuration 1 and Configuration 2 for the numerical simulation. Configuration 3 was excluded due to the unavailability of the spall liner material properties as a part of the simulation code. The projectile was shot at 833 m/s on both the configurations as seen in Figure 4 (a). It was observed for the impact on Configuration 1 the projectile was eroded and failed to penetrate the single armour plate. Thus, no plug formation was observed as seen in Fig. 5.

Configuration 2 was also impacted with the same projectile and velocity. It was observed that the Projectile simply perforates the thin, mild steel bodywork. During the perforation of thin mild steel, the projectile nose shape changes slightly, as seen in Fig. 4(b). It can also be observed that the jacket gets eroded, and the lead core, instead of shattering as observed in the first case, heavily compresses against the armour plate and causes plug formation and the ring of the jacket material ejects alongside the plug as seen in Fig. 6 (a) and (b).

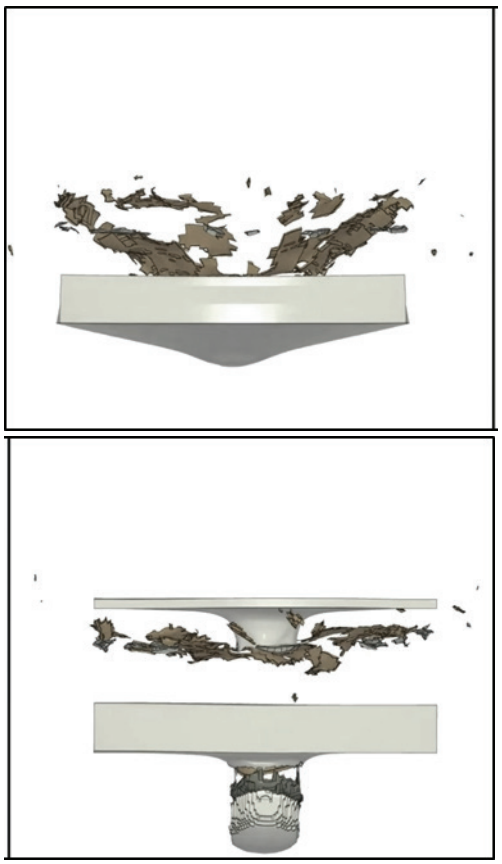

Figure 5. Bulge caused on the single high-hardness armour plate of Configuration 1 and Plugging failure observed in high-hardness armour plate of Configuration 2.

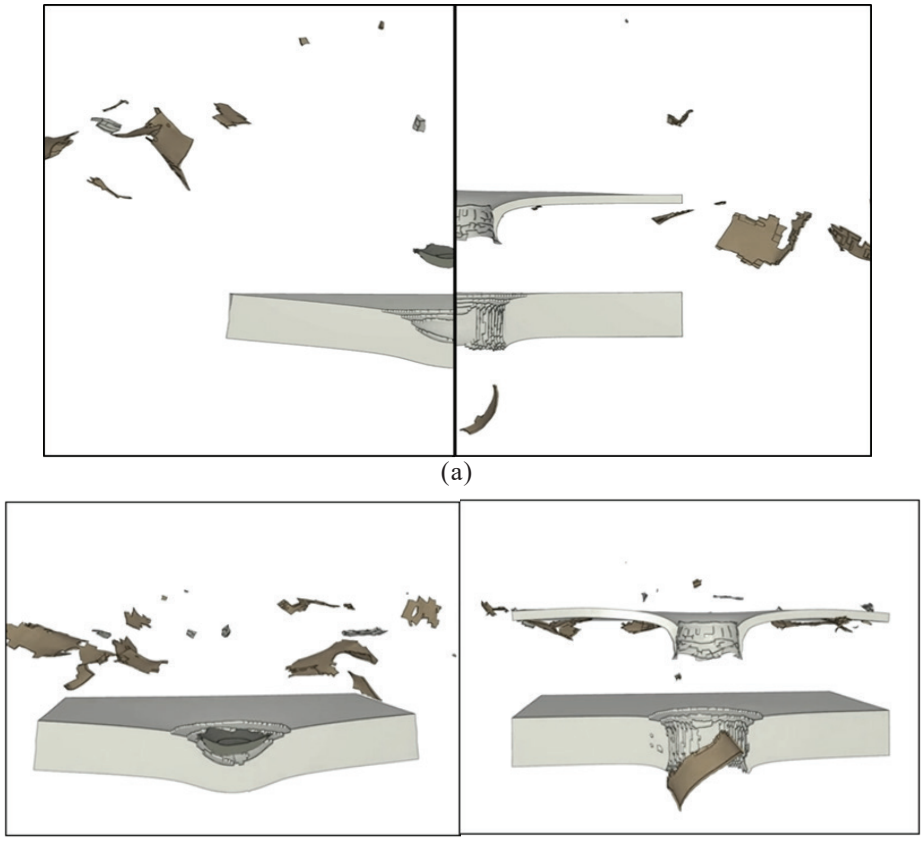

Figure 6. (a) Bulge caused in the Configuration 1 and complete perforation observed in the Configuration 2; and (b): Bulge caused in the Configuration 1 and full perforation observed in the Configuration 2.

The failing armour plate's observations revealed an exceptional vulnerability to adiabatic shear localization, a thermo-viscoplastic instability. Temperature and triaxiality, are both important variables affecting the localization of deformation and, thus, the adiabatic shear localization. The failure model must take stress triaxiality into account since it is vital for adiabatic shear localization, which is connected to the macroscopic plugging penetration process.

After perforating the bodywork, the impact on the armour plate generates a high-pressure shock wave that rapidly compresses it. This compression work leads to an increase in temperature, known as adiabatic heating – the armour plate experiences adiabatic heating due to the compression caused by the projectile's impact. The shock wave generated by the effects rapidly increases the pressure on the armour plate, leading to adiabatic compression and subsequent adiabatic heating of the material. The temperature rise in the armour plate can affect its mechanical properties and response to the impact – the adiabatic heating of the armour plate results in localized deformation.

Strain rate and temperature are key factors contributing to adiabatic shear localization during high strain-rate deformation. Adiabatic shear localization occurs under extremely high strain rates that exceed the material's strain rate sensitivity. At high strain rates, the material's flow stress increases, and the ability to dissipate energy decreases. This leads to the concentration of deformation in localized regions. Adiabatic shear localization is also due to adiabatic heating, where the rapid temperature rises within the localized deformation zones. During high strain rate deformation, a significant amount of plastic work is converted into heat due to the inability of the material to dissipate it efficiently.

The combination of high strain rates and adiabatic heating leads to the initiation and propagation of adiabatic shear bands. These localized regions of intense plastic deformation concentrate strain, resulting in significant shear strain and high shear stress within the shear bands leading to localized damage. The plugging mechanism, connected to adiabatic shear localization, is sensitive to stress triaxiality.

4. DISCUSSION

For every shot fired in the second configuration. It was observed that the design was not able to provide the required ballistic protection. The armour steel plate was perforating for every attempt, and the mode of failure followed was plugging failure. When the projectile was perforating the thin mild steel plate, i.e., the bodywork, the projectile changed its shape to blunt, and this blunted projectile contributed to the perforation of the armour steel plate in the form of plugging.

It can also be noted that when the projectile was perforating the bodywork, the thin mild steel material was jacketing the copper jacket of the projectile; hence, the mild steel jacket might be contributing to the shearing failure mechanism in the armour steel plate.

As the mode of failure is plugging. Then it is sure that this is because of the adiabatic shear phenomenon, which can

occur when armour steel is subjected to a high strain rate and high temperature at a localised region of the projectile impact, which can further soften the material and lead to plugging.

Localised deformation in high-hardness ballistic steel results in the characteristic plugging failure, which is influenced by the local stress-triaxiality ratio and adiabatic heating of the material. These two variables also have a significant impact on the failure of the configuration.

The reasons mentioned are contributing to the failure of the configuration, i.e., thin mild steel bodywork plus Armox 500T armour steel plate with airgap in between, which can be termed the "bodywork effect," where the ballistic resistance offered by the configuration is less as compared to the single Armox 500T armour steel plate.

5. CONCLUSION

The bodywork effect has been investigated in the experiment against the 7.62×51 mm NATO Ball M80 projectile. This experiment has shown that the projectile geometry change, the projectile nose's jacketing with the mild steel material, adiabatic shear localization, and stress triaxiality contribute to the bodywork effect.

Single high-hardness armour steel provides better ballistic resistance than the configuration where bodywork is mounted over the main high-hardness steel armour.

Therefore, the observed experimental "bodywork effect" phenomenon can be of immense significance to fraternity members developing, testing, and evaluating high-hardness armour steel.

REFERENCES

1. NATO Standardization Agency. Procedures for evaluating the protection levels of logistic and light armoured vehicles for KE and Artillery threats, STANAG NATO 4569 AEP-55, Appendix 1, 2004, **1,** pp. 28-29.
2. Gupta, N.K. & Madhu, V. An experimental study of normal and oblique impact of hard-core projectile on single and layered plates. *Int. J. Impact Eng*., 1997, **19**(5–6), 395-414. doi:10.1016/S0734-743X(97)00001-8
3. Gupta, N.K.; Ansari, R. & Gupta, S.K. Normal impact of ogival nosed projectiles on thin plates. *Int. J. Impact Eng.,* 2001, **25**(7), 641-660. doi:10.1016/S0734-743X(01)00003-3
4. Corran, R.S.J.; Shadbolt, P.J. & Ruiz, C. Impact loading of plates – An Experimental investigation. *Int. J. Impact Eng*., 1983, **1**(1), 3-22. doi:10.1016/0734-743X(83)90010-6
5. Backman, M.E. & Goldsmith, W. The mechanics of penetration of projectile into targets, *Int. J. Eng. Sci.,* 1978, **16**(1), 1-99. doi:10.1016/0020-7225(78)90002-2
6. Tan, V.B.C.; Lim, C.T. & Cheong, C.H. Perforation of high strength fabric by projectiles of different geometry. *Int. J. Impact Eng*., 2003, **28**(2), 207-222. doi:10.1016/S0734-743X(02)00055-6
7. Borvik, T.; Langseth, M.; Hopperstad, O.S. & Malo, K.A. Perforation of 12 mm thick steel plates by 20 mm diameter projectiles with flat, hemispherical and conical noses: Part I: Experimental study. *Int. J. Impact Eng*., 2002, **27**(1), 19-35. doi:10.1016/S0734-743X(01)00034-3
8. Corbett G.G.; Reid S.R. & Johnson W. Impact loading of plates and shells by free-Flying projectiles – A review. *Int. J. Impact Eng*., 1996, **18**(2), 141-230. doi:10.1016/0734-743X(95)00023-4
9. Ben-Dor, G.; Dubinsky, A. & Elperin, T. Ballistic impact: Recent advances in analytical modeling of plate penetration dynamics: A review. *Appl. Mech. Rev.,* 2005, **58**, 357-371. doi:10.1115/1.2048626.
10. Dey, S.; Børvik, T.; Hopperstad, O.S.; Leinum, J. & Langseth, M. The effect of target strength on the perforation of steel plates using three different projectile nose shapes. *Int. J. Impact Eng.,* 2004, **30**(8–9), 1005–1038. doi: 10.1016/j.ijimpeng.2004.06.004.
11. Hou, H.; Chen, C.; Cheng, Y.; Zhang, P.; Tian, X.; Liu, T. & Wang, J. Effect of structural configuration on air blast resistance of polyurea-coated composite steel plates: Experimental studies. *Mater. Des.,* 2019, **182**, 108049. doi:10.1016/j.matdes.2019.108049.
12. Hazell, Paul J. Armour: Materials, theory, and design. CRC Press, Taylor & Francis Group, 2015. doi:10.1201/b18683.
13. Ranaweera, P.; Bambach, M.R.; Weerasinghe, D. & Mohotti, D. Ballistic impact response of monolithic steel and tri-metallic steel–titanium–aluminium armour to nonrigid NATO FMJ M80 projectiles. *Thin-Walled Struct.,* 2023, **182**(Part A), 110200 doi:10.1016/j.tws.2022.110200.
14. Antoinat, L.; Kubler, R.; Barou, J.L; Viot, P.; Barrallier, L. Perforation of aluminium-alloy thin plates. *Int. J. Impact Eng.,* 2015, **75**, 255-267. doi:10.1016/j.ijimpeng.2014.07.017.
15. Iqbal, M.A.; Tiwari, G.; Gupta, P.K. & Bhargava, P. Ballistic performance and energy Absorption characteristics of thin aluminium plates. *Int. J. Impact Eng.,* 2015, **77,** 1-15. doi:10.1016/j.ijimpeng.2014.10.011.
16. Coghe, F.; Kestelyn, B. & Pirlot, M., Experimental validation of the origin of the bodywork effect (K-effect) in the up-armouring of civil and military vehicles. 24th International Symposium on Ballistics, New-Orleans, Louisiana, September 2008. pp. 421-429.
17. Nsiampa, N.; Coghe, F. & Dyckmans, G. Numerical investigation of the bodywork effect (K-effect). *In* Proceedings of the Ninth International Conference on the Mechanical and Physical Behavior of Materials Under Dynamic Loading, Brussels, Belgium, EDP Sciences, Brussels, Belgium, 2009. pp. 1561-1569. doi:10.1051/dymat/2009220.
18. Coghe, F.; Nsiampa, N.; Rabet, L. & Dyckmans, G. Experimental and numerical investigations on the origins of the Bodywork Effect (K-Effect). *J. Appl. Mech.,* 2010, **77**(5), 051801.

doi:10.1115/1.4001692.
19. Cimpoeru, S.J. The Mechanical Metallurgy of Armour Steels, Land Division, Defence Science and Technology Group, 2016, pp. 18-21.
20. Popławski, Arkadiusz.; Kędzierski, Piotr & Morka, Andrzej. Identification of Armox 500T steel failure properties in the modeling of perforation problems. *Mater. Des.,* 2020, **190,** 108536. doi:10.1016/j.matdes.2020.108536.
21. SSAB, SSAB in brief. https://www.ssab.com/company/about-ssab/ssab-in-brief. (Accessed on 26th June 2023).
22. Armox500T, Armox 500T general product description, https://www.ssab.com/en/brands-and-products/armox/product-offer/armox-500t . (Accessed on 26th June 2023).
23. Johnson, G.R. & Cook, W.H. A constutitive model and data for metals subjected to large strains, high strain rates and high temperatures. *In* Proceedings of the 7th International Symposium on Ballistics, The Hague, The Netherlands, 1983. pp. 541-547.
24. Iqbal, M.A.; Kasilingam, S.; Sharma, P. & Gupta, N.K. An investigation of constitutive behaviour of Armox 500T Steel and Armour Piercing Incendiary Projectile Material. *Int. J. Impact Engg.,* 2016, **96**, 146-164. doi:10.1016/j.ijimpeng.2016.05.017.
25. Adams, B. Simulation of ballistic impacts on armoured civil vehicles. MT 06.03., Eindhoven University of Technology, The Netherlands. 2006. PhD Thesis.
26. Champagne, V.K.; Helfritch, D.J.; Trexler M.D. & Gabriel, B.M. The effect of cold spray impact velocity on deposit hardness. Modelling Simul. *Mater. Sci. Eng.,* 2010, **18,** 065011. doi:10.1088/0965-0393/18/6/065011

CONTRIBUTORS

Mr Gavhane Viraj Vijaykumar obtained his MTech in Defence Technology with specialisation in Combat Vehicle Engineering from the Amity University, Noida. He is currently working as Assistant Manager – Design and Development at Mahindra Defence Systems Limited, Palwal. His research interests are in the areas of armour materials, and ballistic and blast impact mechanics.
Contribution to the current study: He performed numerical simulations and written an overall manuscript.

Mr Anshul Sharma obtained his MTech in Armament and Combat Vehicles from the Defence Institute of Advanced Technology, Pune. He has been working for Mahindra Defence Systems Limited, Palwal, Haryana and currently working as Manager – Design & Development. His research interests are in the areas of armour materials, composite materials, design and selection, effective ballistic and blast testing, and impact mechanics.
Contribution to the current study: He supervised overall manuscript, performed experiments, and evaluated the experimental results.

Dr Srinivasa Rao Gorrepati is working as an Assistant Professor at the Amity University, Noida. He obtained his PhD from Jawaharlal Nehru Technological University, Kakinada, Andhra Pradesh. His research interests are in the areas of materials, composites, welding, and corrosion.
Contribution to the current study: He evaluated the numerical results.